Reproducible Surface Extraction for Variance Comparison in 3D Computed Tomography

Christoph Heinzl[1], Johann Kastner[1] and Eduard Gröller[2]

[1] Upper Austrian University of Applied Sciences,
Stelzhamerstrasse 23, A-4600 Wels, Austria
[2] Vienna University of Technology, Institute of Computer Graphics and Algorithms,
Karlsplatz 13, A-1040 Vienna, Austria

Abstract. This paper describes a novel method for creating surfaces models from distorted volume datasets in 3D computed tomography (3D-CT). As all 3D-CT datasets are prone to artefacts, especially geometry extraction may produce erroneous surface models if a single global threshold is used. Depending on the selected threshold either the area of material is thickened because ambient noise is added (threshold too low) or it is thinned because outlying material regions are classified as air (threshold too high).We propose a pipeline model which creates a reproducible output using common 3D image processing filters: First of all we use an edge preserving diffusion filter to reduce noise without blurring the edges of the specimen. Furthermore, a watershed segmentation filter is applied to the gradient image in order to extract a binary volume of the dataset. In the final step the surface model is constructed using an advanced approach called elastic surface nets. The major contribution of this paper is the development of the specific processing pipeline for extracting surface models of homogeneous industrial components and to handle large resolution data of industrial CT scanners. The pipeline is crucial for the following visual inspection of deviations.

Introduction

Non Destructive Testing (NDT) is a very common means of quality assurance in modern engineering. The advantages of this way of examining a specimen are obvious: the specimen does not get destroyed and therefore several different testing methods can be applied on the same specimen.

In the area of dimensional measurement typically tactile methods like coordinate measuring are widely used. In recent years coordinate measuring is supported by optical methods, which are able to generate a pointcloud of surfacepoints representing the original surface. But tactile and optical methods have one major disadvantage: internal features can not be measured. For providing the full geometric information of a specimen, the importance and applicability of 3D computed tomography (3D-CT) is increasing. 3D-CT is a radiographic NDT method to locate and size volumetric details in three dimensions. A 3D-CT scanner generates a series of X-ray attenuation measurements, which are used to produce a 3D grid of greyvalues directly corresponding to the spatial density information [12]. The quality of a 3D-CT measurement is exposed to several influencing factors, which

produce artificial structures in the resulting dataset. These structures are called artefacts. The characteristics of artefacts depend on environmental conditions of the measurement. Some aspects which directly influence the extent and size of artefacts are: the specimen's material and geometry, penetration lengths, positioning of the specimen in the ray, the measurement parameters [7].

Dimensional measurement and variance comparison are well established methods for geometric comparison tasks used in automobile and consumer industry. For these methods a surface model or a set of crucial dimensions are calculated of the 3D-CT dataset which is compared to reference geometry data. To extract the surface data, usually a single isovalue is specified to distinguish between air and material (see [11]). A polygonal surface mesh is extracted along the selected threshold using a surface creation algorithm. For example the marching cubes algorithm creates triangle models of constant density surfaces from 3D volume data [2]. If a 3D-CT dataset is affected by artefacts the distinction between air and material is more difficult and a single threshold is in most cases not sufficient. At certain locations a thickening of the structure emerges, where in others thinning and deformations are outlined. Examples are pointed out in Figure 1 showing a CT scan of a motorcycle engine piston.

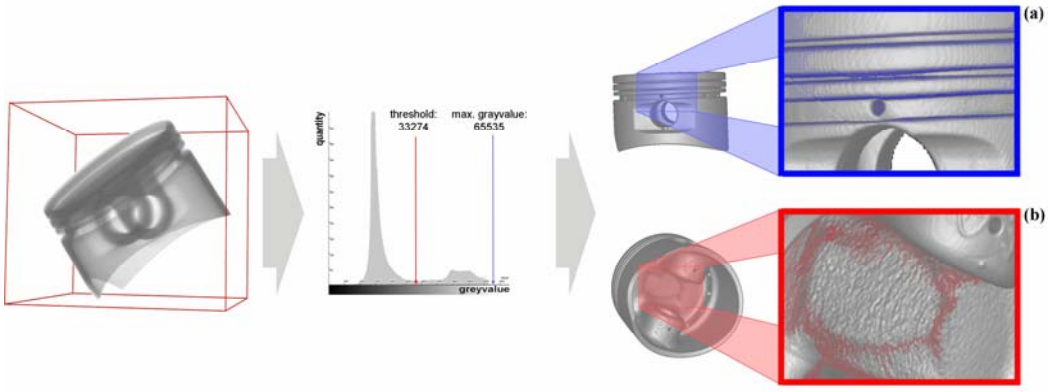

Figure 1: engine piston of a motorcycle, 3D-CT scan, large penetration lengths and complex geometry result in heavy artefacts, specification of a global threshold in the dataset's histogram results in a deformation of the surface model (a) thickening and additional structures, (b) thinning: material is classified as air

Our work concentrates on surface extraction from homogeneous industrial workpieces. In this paper a novel data processing pipeline for the stated problem area is presented, which is robust concerning most artefact types and which is practical in terms of memory and time consumption.

1. Related Work

In order to extract a surface model of a 3D-CT dataset, there are quite a lot of suitable methods to choose. Generally these methods can be separated into two sets: Either the dataset is enhanced in a way, so that a single threshold is sufficient (Section 1.1). Or the dataset is considered as "ground truth" and the best possible surface is extracted (Section 1.2).

1.1 Dataset enhancement

Kasperl [13] proposed an iterative algorithm to reduce scattered radiation and beam hardening in cone beam computed tomography called Iterative Artefact Reduction (IAR). The technique is based on a linearization method which applies a nonlinear characteristic correction curve on the dataset. This curve is directly extracted from the dataset without

having to use a calibration object. Projection images are pre-processed using the correction curve which is extracted from the post-processing step of the reconstruction. So each iteration enhances the correction curve and therefore the quality of the dataset. A related method was introduced by Hopkins et al. [9].

Zauner et al. [16] introduced a method to enhance projection images using platelet filtering. Platelets reduce the ambient noise of projection images using piecewise linear approximations. These approximations are specified by localized functions at various scales, locations, and orientations. The applied platelet representation algorithm is specialized on Poisson noise limited imaging-devices like X-ray detectors.

1.2 Surface extraction

Steinbeiss [14] developed algorithms, which locally adapt the threshold to determine the best local threshold setting. Using an initial, suitable surface model of the specimen, greyvalue profiles are calculated in the direction of each point's surface normal. The vertex location is then adjusted to correspond to the position with maximal gradient magnitude. To minimize the sensitivity to noise in the dataset, neighbouring profiles are considered. Due to averaging of the vertex positions this algorithm is not able to distinguish between noise and very small features.

Bischoff and Kobbelt [6] introduced algorithms on isosurface topology simplification and isosurface reconstruction with topology control. They use a priori knowledge about the topology of the input data to eliminate topological artefacts which are not available in our special application scenario.

A method which extracts a surface model from binary data was proposed by Gibson [5]. This method produces feature-preserving surface models by using a relaxation scheme within predefined constraints. In a large part the quality of this method depends on the prior segmentation. So Gibson's algorithm has to be expanded with a mechanism for artefact reduction, segmentation and binarization. In the presented pipeline model these expansions are introduced.

2. Surface extraction of homogeneous industrial workpieces

Section 2 gives a detailed description of the pipeline model, which is outlined in Figure 2. Generally the use of fully three dimensional image processing filters is crucial, in order to extract as much information from a dataset as possible. If the pipeline were applied on two dimensional slice images of the dataset, all the information of the third dimension would be lost.

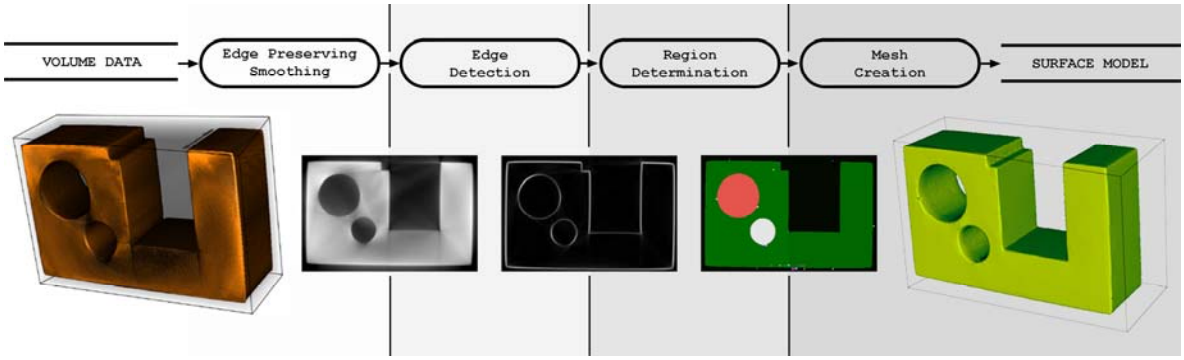

Figure 2: Pipeline for surface extraction of homogeneous industrial workpieces
Input: volume dataset with distorted density values, Output: Surface mesh

2.1 Edge Preserving Smoothing

In order to reduce ambient noise of 3D-CT datasets and to support the subsequent segmentation procedure a smoothing algorithm has to be applied. As standard smoothing filters like Gauss filtering blurs the whole dataset, small image details are lost and edges are moved. Therefore a method is needed which preserves edges and fine details on the one hand, while it smoothes large areas with similar greyvalues on the other hand. Applying an anisotropic diffusion filter, smaller scattered radiation effects and a large part of the ambient noise can be removed. Perona and Malik [3] introduced a method which satisfies these specifications. The basic idea of this anisotropic diffusion scheme is to smooth the dataset while preserving specific image features using partial differential equations. This was done by using the following equations:

$$I_t = div(c(x,y,t)\nabla I) = c(x,y,t)\Delta I + \nabla c * \nabla I \quad (1)$$

$$c(x,y,t) = g(\| \nabla I(x,y,t) \|) \quad (2)$$

I is the dataset to be smoothed, I_t is the evolution of the image over time, div is the divergence operator, ∇ and Δ are gradient and Laplacian operators, $g(\ )$ is a non negative monotonically decreasing function with $g(0)=1$, $c(x,y,t)$ is a decreasing function of the dataset's gradient. If $c(x,y,t)$ is defined as a monotonically descending function, the diffusion will be forced to take place mainly in the interior regions [8]. As ambient noise is higher in 3D-CT datasets of specimens with lower density, we support prefiltering by a platelet based denoising approach. Zauner et al. [16] propose to use platelets to reduce noise of projection images. Platelets reduce the ambient noise of projection images using piecewise linear approximations which are specified by localized functions at various scales, locations, and orientations. A subsequent reconstruction of the CT dataset returns a smoothed but edge preserving dataset. The disadvantage of this method is, that the original projection data has to be accessible and the dataset has to be reconstructed in a time consuming process. Especially for plastics better results can be achieved.

2.2 Edge detection and region determination

After pre-filtering, the gradient magnitudes are calculated by computing the directional derivative at each location of the dataset using a first-order derivative operator. Areas of high local greyvalue deviations are enhanced, which supports the segmentation process. In the presented pipeline model watershed segmentation is used to build up a binary volume. Watershed segmentation is a low-level image analysis algorithm producing a hierarchy of segmented and labelled regions from a scalar-valued input [4]. Treating an image as a height function of greyvalues, a watershed region is characterized by the ridges of neighbouring catchment basins. A catchment basin is defined around each local minimum such that each of its points is connected with the local minimum by a descending path. A flooding level, which floods the height function, reduces oversegmentation and decreases the number of extracted regions. Shallow segments with lower level than the flood levels merge, eroding boundaries of adjacent regions. To classify the regions into material and air, a binarization step is appended. In the binarization step the mean greyvalue of each region is calculated classifying the regions either by a global threshold or a relative threshold to construct the binary volume step by step.

2.3 Mesh creation

To create a globally smooth but feature preserving surface model from the binary dataset Gibson's [5] constrained elastic surface nets algorithm is used. The algortihm identifies surface vertices using volume cells. If every cell corner of a volume has the same binary value, then the volume cell has to be completely inside or completely outside the segmented object. Otherwise a surface cell has been found. In this case a surface vertex is initialized by placing the vertex in the centre of the volume cell. The neighbourhood for each vertex has to be determined. Assuming only face connected neighbour volume cells, each vertex in the volume can have a maximum of six linked neighbour volume cells. A relaxation step modifies the position of each vertex. An energy measure controls the smoothing process in the surface net, which is computed as the sum of the squared lengths of all edges starting from the considered vertex. To retain thin structures, a constraint is defined which forces every vertex to stay within its original volume cell. In the final step the surface is being triangulated.

3. Results and discussion

3.1 General Remarks

CT scans of all workpieces were performed on a HWM Rayscan 250E with a 225 keV microfocus tube. Reference measurements were carried out on a Zeiss Spectrum coordinate measuring machine (accuracy: +/-2,3µm) and a GOM ATOS I/I SO digitizing system. The pipeline was implemented in Visual C++ using the ITK and the VTK libraries. For details on tuning the pipeline and on visualization see [15]. Overall processing times were measured on an Opteron 275 system with 4GB RAM.

3.2 Workpieces

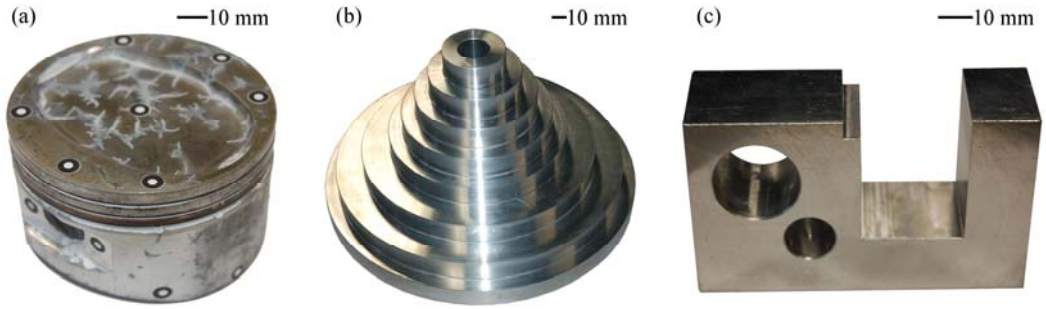

Figure 3: Workpieces: (a) Al-piston of a motorcycle, (b) Al-step cylinder, (c) regular Al-test part

Workpiece one (Figure 3a) is an aluminium engine piston of a motorcycle. Especially on the upper and lower face of the piston as well as on the piston rings severe artefacts appear because of high penetration lengths and scattered radiation. The piston was measured using the following settings: 630 projection images, 200 kV, 500 µA, 500 ms integration time. The X-ray beam was prefiltered using 0.5 mm Cu to reduce low energetic radiation. The resulting 16 bit dataset was 408*351*355 in size with a voxelsize of 281 µm.

Workpiece two (Figure 3b) is an aluminium step cylinder with a drill whole along the longitudinal axis. The step cylinder consists of five concentric rings with increasing diameter. In the lower rings, where penetration lengths are higher, artefacts affect the dataset such that it is difficult to distinguish between material and air. Settings of this

measurement: 720 projection images, 210 kV, 1000 µA, 500 ms integration time, 1 mm Cu prefiltering. These settings resulted in a dataset of 561*559*436 voxels and a voxelsize of 236 µm.

Workpiece three (Figure 3c) is a regular aluminium test part with two drill holes and two rectangular millings (as described by Kasperl in [13]). This object produces severe artefacts due to different material thicknesses and relatively high penetration lengths. The dataset was measured with a voxelsize of 200 µm using 810 projection images at 200 kV, 620 µA, 500 ms integration time and prefilter plates of 0.1 mm Pb and 0.15 mm Cu. The resulting 16 bit dataset had an extent of 339*525*169 voxels.

3.3 Analysis

In Figure 4 the results are shown when applying the pipeline on the motorcycle piston. The axial cross section (a) shows a slice image of the CT-dataset. Artificial structures of the piston pin drill are obvious and furthermore the contrast between air and material greyvalues is very weak in the area of the piston face. Using this input data, global thresholding would produce a distorted surface model. Figure 4(b) points out these circumstances showing a surface model which was created using Otsu's global threshold (see [1]). The resulting surface model is seriously modified in the area of the upper and the lower face of the piston. Another critical area can be found at the piston rings which appear partly closed. Applying our pipeline on this workpiece we succeeded in creating a smooth but feature preserving surface model as shown in Figure (c). The geometry modifications in the lower piston face could be successfully avoided and also the geometry of the piston rings was well extracted. Figure 4 (d) shows a variance comparison between the isosurface with Otsu's threshold and the surface model of the pipeline. The isosurface deviates from our extracted surface model by up to +/- 3.4 mm in artefact affected areas (red areas). The overall processing time for this specimen was 4:26 minutes.

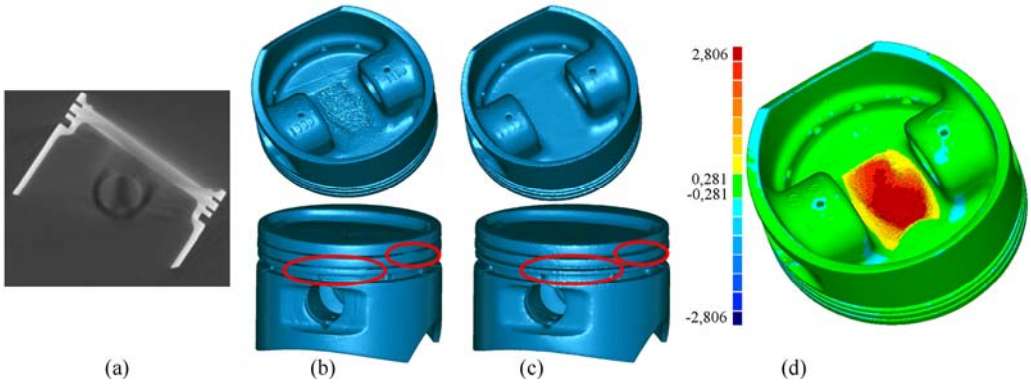

Figure 4: Analysis of piston: (a) axial cross section with artificial structures, (b) best isosurface using Otsu's global threshold method , (c) surface model of pipeline, (d) variance comparison between isosurface and surface model of pipeline

In case of the step cylinder especially the inner and outer diameters of the cylinders are of interest. Figure 5 shows a diagram which plots the deviation to a reference measurement of a coordinate measuring machine versus the diameter of the cylinders. In this diagram the extracted inner and outer diameters of the presented pipeline are compared to the best isosurface. The threshold for this isosurface was selected manually because Otsu's method was not suitable for this dataset. The pipeline produces a nearly linear characteristic for all extracted diameters. Especially the extracted outer diameters are very close to the reference measurement (mean deviation 4,6 µm for outer diameters and 59,5µm for inner diameters). The extracted outer diameters are closer to the reference measurement because the number of relevant sample points is significantly higher and therefore ambient noise can be removed. Otsu's global threshold method is exposed to artefacts. The global threshold is

not ideal for all wall thicknesses, which is pointed out by large deviations in the positive as well as the negative sense. The surface model of this object was extracted in 6:39 minutes

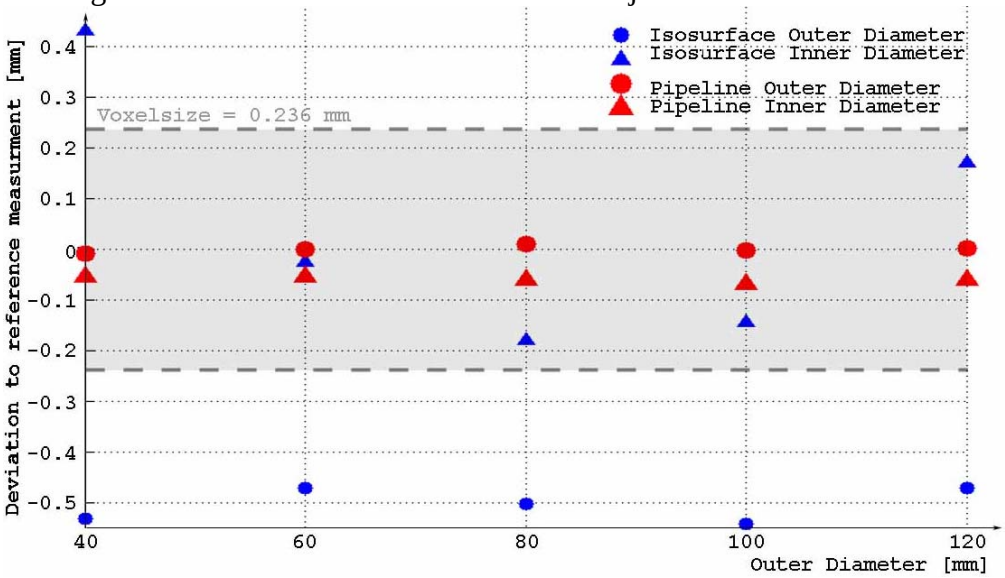

Figure 5: Plot of deviations to reference measurement versus the diameter of the cylinders. Inner and outer diameters of workpiece two are considered. Otsu's global threshold method is compared to the extracted dimensions of the pipeline. Reference measurement was carried out using a coordinate measuring machine.

Workpiece three was designed by Kasperl [13] with the aim of producing severe artefacts to test artefact reduction algorithms (see Figures 3, 6). Artefacts modify the surface especially in the area of the smaller drill hole and along the rectangular millings. Figure 6(b) shows these effects with an isosurface model of the dataset using Otsu's threshold. The colorcoded variance comparison to the optical reference measurement points out large deviations by dark blue and dark red colors (Figure 6(c)). Applying our pipeline on this workpiece a surface model was extracted with an average error of 66µm at a voxelsize of 200µm while the average error of the isosurface using Otsu's method was 216µm. Figure 6c) shows the extracted smooth but feature preserving surface model. Mind the different color codings in (c) and (e): yellow indicates deviations of up to 100µm while dark blue deviations up to 2mm. The pipeline managed to extract the surface model for this object in 3:19 minutes.

4. Summary and conclusions

A new method for surface extraction of homogeneous industrial workpieces is presented, which is robust to a certain extent concerning common artefacts. The presented pipeline model extracts robust and low error surface models, which is crucial for dimensional measurement. The applicability and accuracy has been shown on homogeneous test parts as well as industrial workpieces. Typical dimensional accuracies were 4.6 µm for inner diameters and 59.5 µm for outer diameters of an Al-stepcylinder and 66 µm for the surface of an Al-testpart. Aims of our future work are adding multimaterial support and improving the pipeline's exactness.

5. Acknowledgements

The presented work has been funded by the Austrian Research Promotion Agency's (FFG) FH-Plus Project "Zerstörungsfreie und In-situ-Charakterisierung von Werkstücken und Materialien unter besonderer Berücksichtigung von Brennstoffzellen" and partly supported

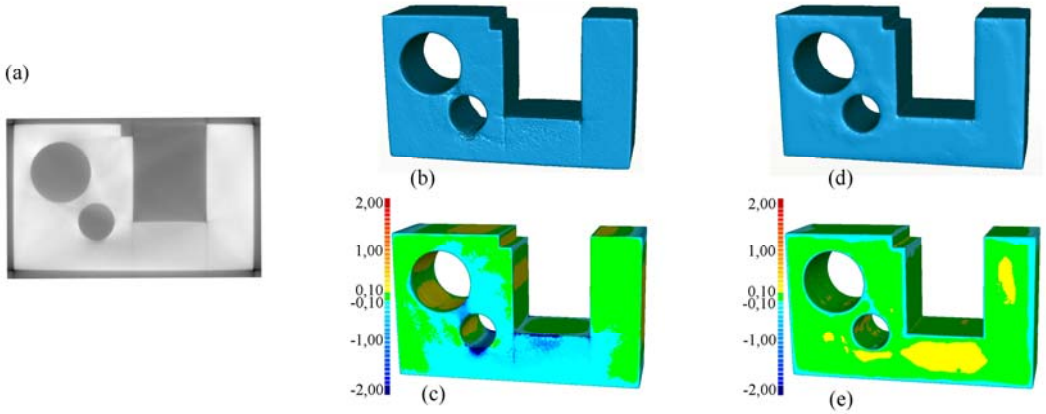

Figure 6: Analysis of workpiece three: axial cross section (a), isosurface using Otsu's threshold (b), variance comparison between isosurface vs. optical reference measurement (c), extracted surface model using our pipeline (d) variance comparison between surface model vs. optical reference measurement

by the PVG project, Austrian Science Fund (FWF) grant no P18547-N13. Thanks to Matej Mlejnek and the visgroup of the Vienna University of Technology for support in designing the pipeline and to Roman Klingesberger and CT group of the Upper Austrian University of Applied Sciences for illustrations, CT and reference measurements.

References

[1] N. Otsu, A threshold selection method from grey level histograms, IEEE Transactions on Systems, Man, and Cybernetics, Vol. 9, 1979

[2] Lorensen, W. and Cline, H., Marching cubes: A high resolution 3D surface construction algorithm, ACM SIGGRAPH Computer Graphics, vol. 21, p.p. 163-169, 1987

[3] Perona, P. and Malik, J., Scale-space and edge detection using anisotropic diffusion, Transactions on Pattern Analysis and Machine Intelligence, vol. 12, p.p. 629-639, 1990

[4] Vincent, L. and Soille, P., Watersheds in Digital Spaces: An Efficient Algorithm based on Immersion Simulations, IEEE Transactions on Pattern Analysis and Machine Intelligence, vol. 13, no. 6, 1991

[5] Gibson, S.F.F., Constrained Elastic Surface Nets: generating smooth surfaces from binary segmented data, Lecture Notes in Computer Science, vol. 1496, p.p. 888-898, 1998

[6] Bischoff, Stephan and Kobbelt, Leif, Isosurface Reconstruction with Topology Control, Pacific Conference on Computer Graphics and Applications, p.p. 246-255, 2002

[7] Hsieh, J., Computed Tomography: Principles, Design, Artifacts and Recent Advances, SPIE-The International Society for Optical Engineering, 2003

[8] Ibanez, L. and Schroeder, W., The ITK Software Guide, Kitware, Inc., 2003

[9] Hopkins, F., Du, Y., Lasiuk, B., Abraham, A. and Basu, S., Analytical correcions for Beam-Hardening and object scatter in volumetric computed tomography systems, Proceedings of WCNDT 2004, p.p. 462-468, Montreal Sept 2004

[10] Schroeder, W. and Martin, K. and Lorensen, B., The Visualization Toolkit, Kitware, Inc., 2004

[11] VolumeGraphics, VG Studio Max 1.2 - User's Manual, 2004

[12] Kastner, J., Schlotthauer, E., Burgholzer, P. and Stifter, D., Comparison of X-ray computed tomography and optical coherence tomography for characterisation of glass-fibre polymer matrix composites, Proceedings of WCNDT 2004, p.p. 71-79, Montreal Sept 2004

[13] Kasperl, S., Qualitätsverbesserungen durch referenzfreie Artefaktreduzierung und Oberflächen-normierung in der industriellen 3D-Computertomographie, PhD thesis, Universität Erlangen Nürnberg, 2005

[14] Steinbeiss, H., Dimensionelles Messen mit Mikro-Computertomographie, PhD thesis, Technische Universität München, 2005

[15] Heinzl, C., Klingesberger, R., Kastner, J. and Gröller, E., Robust Surface Detection for Variance Comparison and Dimensional Measurement, Eurographics/IEEE-VGTC Symposium on Visualization, 2006, (to appear)

[16] Zauner, G., Reiter, M., Salaberger, D. and Kastner, J., Denoising of computed tomography images using multiresolution based methods, Proceedings of ECNDT, Berlin Sept 2006, (to appear)